Introduction to Intermolecular Forces

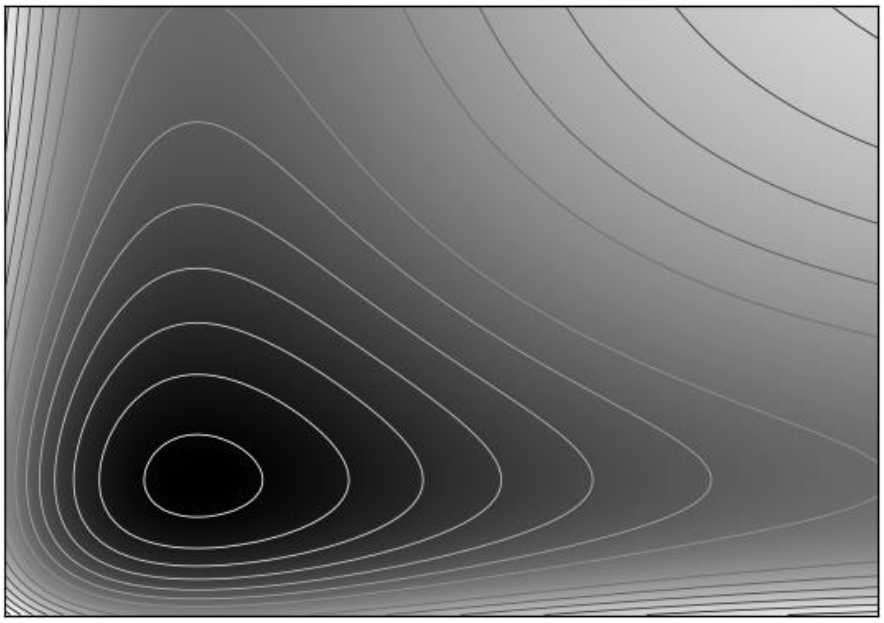

Rubén Thor Wenzel Argüelles
Trabajo de Fin de Grado – Universidad de La Laguna
2018

Under the supervision of Prof. José Diego Bretón Peña.

Summary

The main scope of this work is to explore the fundamental theoretical treatment of intermolecular forces of interaction between atoms and molecules and some of the mathematical approaches employed in the representation of these interactions, and to apply these techniques to evaluate the intermolecular forces in certain atomic and molecular systems.

The material is presented firstly through an introductory assertion of some of the basic ideas applied in the next sections, followed by a comprehensive theoretical exposition of the aspects most relevant to the electromagnetic and quantum mechanical understanding of intermolecular forces, presented in the same manner as done by A. Stone [1]. In the third section the mathematical models that are historically and practically relevant are reviewed, and these are then tested computationally in the fourth section to provide an overall picture of their validity and accuracy at representing the energy of interaction between closed electron shell atoms and ions. The fifth section includes the conclusions drawn throughout the project. Finally, due acknowledgements are given and a list of the references and bibliography employed is included.

This field of study is encompassed in the area of atomic and molecular physics, yet it is relevant in many other disciplines. The reader should be sufficiently accustomed to the principles of physics, mathematics and chemistry and particularly to quantum mechanics to adequately follow the discussion.

As to the author, the development of this work has required many academic competences presented in the courses that deal with the following subjects: Python language, Computational Physics, Electromagnetism, Quantum Mechanics, Atomic and Molecular Physics and Condensate Matter Physics.

CONTENTS

1 Introduction

1.1 A brief historical approach

The idea of a composite world made up of physically indivisible particles of minute size first arose with Democritus, a Greek philosopher, around the 4th century BCE. Later on, the Roman poet and philosopher Lucretius transmitted the ideas of Epicureanism, proposing that the static macroscopic bodies were composed on a small scale by rapidly moving atoms bouncing off each other. These assessments on the nature of matter were apparently long forgotten in European scientific history until the first experimental evidence for the corpuscular composition of matter appeared at the end of the 18th century.

Modern atomic thinking developed throughout the last centuries, resting on the investigations of John Dalton concerning the atomic theory in chemistry (1812), the earlier discovery of Boyle's law (1662), Charles Law (1787) and Gay-Lussac's law (1809) on the proportionalities of the volumes, temperatures and pressures of gases, and later Avogadro's Law (1811) on the proportionality of a gas' volume to the number of particles. The success of these observations led to the development of the Kinetic Theory of Gases in the middle of the 19th century with the work of Rudolf Clausius (1857), although earlier pioneers[1] were neglected by their contemporaries. With the advent of Faraday's laws of electrolysis and the stoichiometry of many chemical reactions, the idea of atoms and molecules as the basic components of matter became consolidated. Further developments in the 20th century like x-ray diffraction or high resolution microscopy (STM or AFM), have reported copious evidence of the atomic and molecular characteristics of matter.

1.2 Physical basis of intermolecular forces

Following this trend of thinking the understanding of forces of interaction between atoms and molecules arose naturally, especially so when considering the existence of condensed

[1] : D. Bernoulli (1738), R. J. Boskovich (1745), M. Lomonosov (1747), G. L. Le Sage (1780), J. Herapath (1843), J. J. Waterston (1843) and A. Krönig (1856) theorized extensively on the kinetic theory of gases.

phases of matter which display evident attractive forces between atoms and molecules. Furthermore, the finite density of matter and difficulty in compressing it shows that at short range these intermolecular forces become repulsive.

Consequently, one may propose that the energy of interaction between two molecules as a function of the distance that separates them must take the form shown in Fig. 1.1, with a long range attractive region and a steeply repulsive region at short range accounting for the aforementioned phenomena. There's a minimum in the energy of interaction at a distance R_m, the depth of this attractive well is symbolized by ε. These features are general to all molecular interactions, yet the form of the function U(R) depends on the particular molecules concerned.

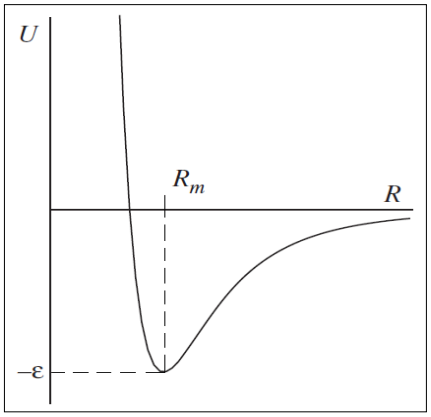

Fig 1.1. General picture of the intermolecular potential energy

Van der Waals first took these ideas into account when describing real gases. He suggested that the incompressibility of the molecules could be expressed as a fixed volume b, a consequence of molecules being undeformable, and that the attractive forces between molecules effectively reduced the pressure of a gas on its container by a factor a, proportional to the square of the density. The gas law then took the form $(P + a\ /\ V^2)(V - b) = RT$, which gives a considerably good account of the condensation of gases into liquids and the constants a and b correspond well enough with the properties of molecules in view of modern understanding.

The parameter ε can be thought of as being approximately the energy required to separate a liquid condensate into its constituent molecules for each pair of adjacent molecules, and it is typically in the region $1 - 260\ meV$. It is considerably weaker than the energy of dissociation of a chemical bond which is greater than $2000\ meV$. Also, the parameter R_m is affected by the attractive forces of distant molecules, effectively compressing adjacent molecules closer and making direct measurement unviable, as opposed to the Van der Waals parameter b which can be obtained through direct methods and can give a reasonable first estimation of the distances of equilibrium R_m. These are usually in the range of $2 - 4$ Å, comparatively bigger with respect to chemical bonds which are of the order of 1 Å.

1.2.1 Origin and classification of intermolecular forces

The forces involved in molecular interactions, as well as the ones involved in the bonding of atoms that make up molecules, are ultimately due to the electromagnetic interaction. The main difference between the physical phenomena that comprises molecular interactions [2] is the distance at which these forces become relevant, thus they can be seen as either long range or short range interactions.

[2] The term molecule will be taken to mean atoms and molecules in the following discussion.

The long range interactions, which also appear in short range but persist at larger distances, have a functional energy of the form $U \sim R^{-n}$. The most relevant contributions are:

I. Electrostatic, which originate from the classical interaction of static charge distributions or permanent multipoles of a pair of molecules. They can be either attractive or repulsive, but they are strictly pairwise additive.

II. Induction. This effect comes into being from the distortion of a particular molecule in the electric field of all its neighbours. Because these fields may reinforce or cancel out each other, this effect is strongly non-additive and it is always attractive.

III. Dispersion is not classically defined, as it arises from to the fluctuation in the charge distribution of the molecules as electrons fluctuate around due to their quantum-mechanical nature.

Besides these main contributions to intermolecular forces, there are other minor contributions: when at least one of the molecules is in an excited state *resonance interactions* also appear, there are also *magnetic interactions* of very small magnitude whenever both molecules have unpaired spins or there are nuclei with non-zero spin. Given that long range interactions are described in terms of power series in R^{-1} these diverge when $R \rightarrow 0$, so they are only valid for large separations even if they are still present at short ranges.

At short range, when the molecular wavefunctions overlap significantly, the electron exchange between molecules plays an important role and the repulsion energy between them behaves as $U \sim e^{-\alpha R}$. Quantum-mechanical effects of approximately additive nature dominate at this stage given that the electron wavefunctions become wider as a result of this overlapping, thus the momentum distribution compresses and an attraction between the molecules appears in favour of this lower energy configuration. However, considering that electrons are fermionic matter, their wavefunctions require Pauli antisymmetry, maintaining this constraint requires energy and acts overall as a repulsive force. The latter becomes the dominant term and the exchange is overall repulsive. Hence the name exchange-repulsion forces.

There are also exchange-induction and exchange-dispersion contributions arising from wave function overlap that dampen the energy of interaction and act as attractive forces. Charge transfer effects are thought of as exchange-induction effects and are non-additive.

1.2.2 Intermolecular forces between several molecules

The energy of interaction in an *n*-molecule system can only be approximately thought of as a pairwise addition of the energies of interaction between the molecules. The reality of the situation is that including an extra molecule to a system alters the overall energy of interaction between any pair of molecules in the system. In other words, if we view the energy of interaction between the molecules as a series U and the energy of any isolated molecule i as W_i, the energy of the assembly would be:

$$W = \sum_i W_i + U = \sum_i W_i + \sum_{i>j} U_{ij} + \sum_{i>j>k} U_{ijk} + \sum_{i>j>k>l} U_{ijkl} + \cdots$$

Thus for each pairwise addition of the interaction of *m* molecules within the *n*-body system, an *m+1* correction to the energy appears. Even though these terms are increasingly smaller, they can't be altogether neglected, the three-body terms may become too large to ignore. However, this approximation is good enough in most situations if the pairwise interaction is properly described.

The equilibrium geometry is altered by the presence of nearby molecules, this departure from equilibrium may be altogether energy efficient. The difference between equilibrium and distorted geometry is known as *deformation energy*, and it constitutes a complicated many-body effect which is usually neglected completely.

1.3 Representation of intermolecular forces

The intermolecular *potential energy curve* (PEC) displayed in **Fig. 1.1** shows the behaviour of the interaction energy between two atoms as a function of the separation between them but for more complicated systems the intermolecular potential is more adequately described as a multidimensional surface, or hyper-surface, which is known as a *potential energy surface* (PES).

To visualize the interaction potential when there are more than two degrees of freedom can only be achieved three-dimensionally by means of a reduced representation. Taking the vertical dimension as the energy of interaction and the two horizontal dimensions as representative of the six or more coordinates that are in use, the PES thus becomes a surface which may be explored as a landscape with hills and valleys, illustrating the possible energy configurations as a function of the relative positions.

If we consider the molecules as rigid bodies these PES are dependent on the set of generalised coordinates $\{q_i\}$ that represent the degrees of freedom available to the molecules, these being translations in space or rotations around the molecule's origin of coordinates. However, the molecular properties on which the intermolecular forces depend are affected by the vibrational degrees of freedom of the molecules, hence coupling may arise between intermolecular and intramolecular motions leading to changes to the vibrational frequencies and to the equilibrium angles and lengths of the bonds between molecules. In this work non-vibrating molecules will be considered so these effects will not be taken into account.

To better understand these PES, it is worthwhile going into how the coordinate systems are constructed and how the degrees of freedom are defined in terms of these. A 'global' coordinate system referenced by Cartesian axes may be employed when there's more than one molecule. This global frame *{X, Y, Z}* is defined, for example, in reference to macroscopic

features, it is fixed in space and relates molecules to each other through translations and rotations. It is also possible to define local or molecular frames of reference by attaching a set of coordinate axes *{x, y, z}* to each molecular centre, taking the z axis along the symmetry axis of the molecule, the x axis perpendicular to the molecular plane and the y axis forming a right-handed orthogonal set. In order to illustrate the degrees of freedom of a system let's consider two characteristic examples:

- In the case of an atom interacting with a linear molecule we can set a global frame with the Z axis through the linear molecule's symmetry axis and originating at the centre of mass, and define the atom's position in terms of the variable $\vec{R}$, which symbolizes the separation between the molecule and atom, and two angular variables (θ, φ) referring to the orientation of $\vec{R}$, as shown in **Fig. 1.2**. This arrangement implies 3 degrees of freedom. By taking a frame of reference tied to the molecule, which in this case implies fixing the atom in the XZ plane, the PES obviously becomes independent of the angular variable φ and $U = U(R, \theta)$.

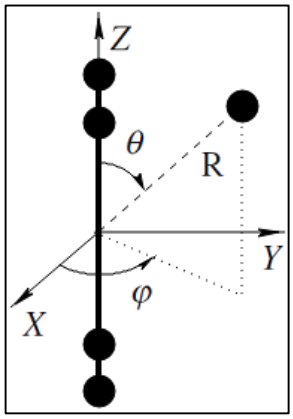

Fig. 1.2. Linear molecule interacting with an atom.

- For two non-linear molecules and by reference to a global frame, each molecule requires a set of Euler-angle rotations (α, β, γ) to define its orientation, which correspond to rotations around the Z, X' and Z'' axes respectively, and three Cartesian coordinates to define its position, making a total of 12 degrees of freedom. If the global Z axis is set through the system's centre of mass and the positions of the molecules are defined by a vector $\vec{R}$ that joins both molecular centres, the degrees of freedom are reduced to 7. This is shown in **Fig. 1.3**. Furthermore, due to the symmetry of the system in the XY plane, the dependency of the PES on the Euler angles α_1 and α_2 may be expressed as $\alpha = \alpha_2 - \alpha_1$ and the degrees of freedom reduced to 6. Therefore, the potential is defined by $U = U(R, \alpha, \beta_1, \gamma_1, \beta_2, \gamma_2)$.

  For a system comprised of A atoms, $N > 2$ molecules, of which L are linear, the number of intermolecular degrees of freedom are $6(N-1) - L + 3A$.

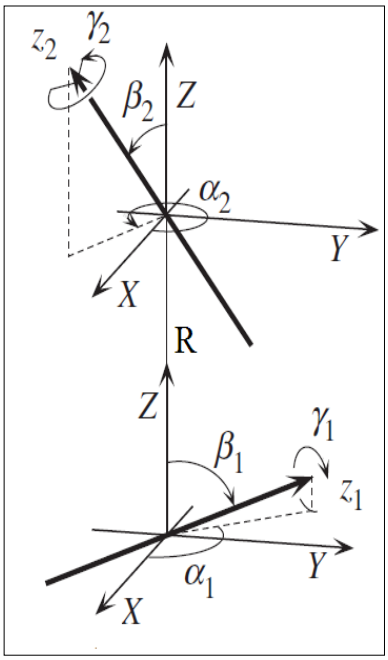

Fig. 1.3. Two non-linear molecules interacting. The global Z axis is presented as well as the local axes z_1 and z_2.

2 Theoretical models

As mentioned in section 1.2, the electromagnetic interaction is the most prominent contribution to the energy of interaction. All the interactions that contribute to define the PES ultimately come from the Coulombic interaction, except for the magnetic terms which are less relevant. Therefore, in describing these interactions there arises the need to define how charge is distributed in a molecule and to do so independently for long and short range contributions to the interaction energy, in compliance with the distinctions that have already been established.

2.1 The electric field created by a molecule

With the aim of obtaining the precise form of the potential energy $U\{q_i\}$, let us start by considering the energy of electrostatic interaction between two molecules. Taking as reference **Fig. 2.1**, the electrostatic potential generated at a point $\vec{R}_B$ by discrete charge distributions e_a which are around a position $\vec{a} + \vec{R}_A$ relative to a global frame of reference has the form:

$$V^A(\vec{R}_B) = \sum_a \frac{e_a}{4\pi\varepsilon_0 |\vec{R}_B - \vec{R}_A - \vec{a}|} = \sum_a \frac{e_a}{4\pi\varepsilon_0 |\vec{R} - \vec{a}|} \qquad (2.1.1)$$

and the electrostatic potential energy of interaction created by discrete charge distributions is:

$$\mathcal{H}' = \sum_{a,b} \frac{e_a\, e_b}{4\pi\varepsilon_0 |\vec{R} + \vec{b} - \vec{a}|} \qquad (2.1.2)$$

when written in terms o f the charge densities $\rho^A(\vec{a}, \vec{R}_A)$ and $\rho^B(\vec{b}, \vec{R}_B)$ centred about $\vec{R}_A$ and $\vec{R}_B$ it becomes [1]:

$$\mathcal{H}' = \iint d\vec{a} d\vec{b} \frac{\rho^A(\vec{a}, \vec{R}_A)\rho^B(\vec{b}, \vec{R}_B)}{4\pi\varepsilon_0 |\vec{R} + \vec{b} - \vec{a}|} \qquad (2.1.3)$$

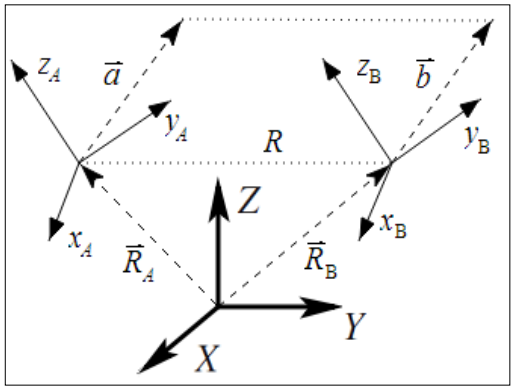

Fig. 2. 1 Two interacting molecules *A* and *B*.

2.2 Long-range molecular interactions

It is most common to express the electrostatic potential as a convergent multipolar expansion when the intermolecular separation is large. The different multipolar moments generated by molecule A appear explicitly in the multipolar expansion for the potential generated by such molecule.

By taking a Taylor series expansion about $\vec{R}_A$ and making use of the tensor notation, Einstein summation convention[3] and other relations[4], the potential (2.1.1) becomes:

$$V^A(\vec{R}_B) = \sum_a \frac{e_a}{4\pi\varepsilon_0}\left\{\frac{1}{\mathrm{R}} + a_\alpha\left(\frac{\partial}{\partial a_\alpha}\frac{1}{|\vec{R}-\vec{a}|}\right)_{\vec{a}=0} + \frac{1}{2}a_\alpha a_\beta\left(\frac{\partial^2}{\partial a_\alpha \partial a_\beta}\frac{1}{|\vec{R}-\vec{a}|}\right)_{\vec{a}=0} + \cdots\right\}$$

$$= \sum_a \frac{e_a}{4\pi\varepsilon_0}\left\{\frac{1}{\mathrm{R}} - a_\alpha\left(\frac{\partial}{\partial R_\alpha}\frac{1}{|\vec{R}-\vec{a}|}\right)_{\vec{a}=0} + \frac{1}{2}a_\alpha a_\beta\left(\frac{\partial^2}{\partial R_\alpha \partial R_\beta}\frac{1}{|\vec{R}-\vec{a}|}\right)_{\vec{a}=0} - \cdots\right\}$$

$$= \sum_a \frac{e_a}{4\pi\varepsilon_0}\left\{\frac{1}{\mathrm{R}} - a_\alpha\nabla_\alpha\frac{1}{\mathrm{R}} + \frac{1}{2}a_\alpha a_\beta\nabla_\alpha\nabla_\beta\frac{1}{\mathrm{R}} - \cdots\right\}. \qquad (2.2.1)$$

in this expression we can identify the zeroth-order moment term as the total charge of molecule A, $\widehat{M} = \sum_a e_a = q$; the first-order moment term is the dipole moment $\widehat{M}_\alpha = \sum_a e_a a_\alpha = \hat{\mu}_\alpha$ and the second-order moment is the quadrupole moment [5] $\widehat{M}_{\alpha\beta} = \sum_a e_a a_\alpha a_\beta = \sum_a e_a\left(a_\alpha a_\beta - \frac{1}{3}a^2\delta_{\alpha\beta}\right) = \frac{2}{3}\Theta_{\alpha\beta}$. The same rules apply for the higher order moments.

With this in mind we rewrite the electrostatic potential as:

$$V^A(\vec{R}_B) = Tq^A - T_\alpha\hat{\mu}_\alpha^A + \frac{1}{3}T_{\alpha\beta}\widehat{\Theta}_{\alpha\beta}^A - \cdots + \frac{(-1)^n}{(2n-1)!!}T_{\alpha\beta\ldots\nu}^{(n)}\hat{\xi}_{\alpha\beta\ldots\nu}^{A(n)} + \cdots \qquad (2.2.2)$$

where, in general:

$$T_{\alpha\beta\ldots\nu}^{(n)} = \frac{1}{4\pi\varepsilon_0}\nabla_\alpha\nabla_\beta\ldots\nabla_\nu\frac{1}{\mathrm{R}} \qquad (2.2.3)$$

are the corresponding Cartesian components of the so called interaction tensors T. The subscripts α, β, γ, etc. can each be x, y *or* z, and the definition of the Cartesian interaction tensors T employs Kronecker deltas for mathematical economy.

---

[3] Any repeated subscript entails a summation over the system's coordinate axes, so: $f_\alpha = f_x + f_y + f_z$

[4] $\frac{\partial}{\partial x}\frac{1}{|\vec{R}-\vec{r}|} = \frac{\partial}{\partial x}\frac{1}{\sqrt{(X-x)^2+(Y-y)^2+(Z-z)^2}} = -\frac{\partial}{\partial X}\frac{1}{|\vec{R}-\vec{r}|}$ The same is true for coordinates y and z.

[5] Such a definition is necessary since the dependence on $1/R$ satisfies Laplace's equation and so there is no contribution to the potential from the trace $M_{\alpha\alpha}$. Permutation of the subscripts doesn't change the value.

We see how convenient this notation is when the operations entailed are carried out:

$$4\pi\varepsilon_0 T = \frac{1}{\mathrm{R}} \tag{2.2.3.1}$$

$$4\pi\varepsilon_0 T_\alpha = -\frac{R_\alpha}{\mathrm{R}^3} \tag{2.2.3.2}$$

$$4\pi\varepsilon_0 T_{\alpha\beta} = \frac{3R_\alpha R_\beta - R^2\delta_{\alpha\beta}}{\mathrm{R}^5} \tag{2.2.3.3}$$

$$4\pi\varepsilon_0 T_{\alpha\beta\gamma} = -\frac{15R_\alpha R_\beta R_\gamma - 3R^2\left(R_\alpha\delta_{\beta\gamma} + R_\beta\delta_{\alpha\gamma} + R_\gamma\delta_{\alpha\beta}\right)}{\mathrm{R}^7} \tag{2.2.3.4}$$

This notation allows to easily determine not only the contributions to the potential from the permanent multipoles of molecule A, but also the electric field $F_\alpha^A\left(\vec{R}_B\right) = -\nabla_\alpha V^A\left(\vec{R}_B\right)$, the field gradient $F_{\alpha\beta}^A\left(\vec{R}_B\right) = -\nabla_{\alpha\beta} V^A\left(\vec{R}_B\right)$ and successive higher derivatives created by its charge distribution.

Thus, returning to equation (2.2.2), the α components of the electric field and field gradient at $\vec{R}_B$ created by the potential $q^A T$ that arises from the charge q^A are as follows:

$$F_\alpha^A\left(\vec{R}_B\right) = -q^A T_\alpha \quad ; \quad F_{\alpha\beta}^A = -q^A T_{\alpha\beta} \tag{2.2.4.1}$$

In the case of the dipolar moment $\hat{\mu}_\gamma^A$, the potential it produces is $-\hat{\mu}_\gamma^A T_\gamma$ and the electric field and field gradient take the following form:

$$F_\alpha^A = \hat{\mu}_\beta^A T_{\alpha\beta} \quad ; \quad F_{\alpha\beta}^A = \hat{\mu}_\gamma^A T_{\alpha\beta\gamma} \tag{2.2.4.2}$$

By taking these relations, the higher order derivatives and equations (2.2.2) and (2.2.3), into account, the electrostatic interaction energy can be written in terms of the multipolar expansion, giving:

$$\begin{aligned}\mathcal{H}' = q^B V^A - \hat{\mu}_\alpha^B F_\alpha^A + \frac{1}{3}\widehat{\Theta}_{\alpha\beta}^B F_{\alpha\beta}^A + \cdots &= q^B\left(Tq^A - T_\alpha\hat{\mu}_\alpha^A + \frac{1}{3}T_{\alpha\beta}\widehat{\Theta}_{\alpha\beta}^A - \cdots\right) \\ &+ \hat{\mu}_\alpha^B\left(T_\alpha q^A - T_{\alpha\beta}\hat{\mu}_\beta^A + \frac{1}{3}T_{\alpha\beta\gamma}\widehat{\Theta}_{\beta\gamma}^A - \cdots\right) \\ &+ \frac{1}{3}\widehat{\Theta}_{\alpha\beta}^B\left(T_{\alpha\beta}q^A - T_{\alpha\beta\gamma}\hat{\mu}_\gamma^A + \frac{1}{3}T_{\alpha\beta\gamma\delta}\widehat{\Theta}_{\gamma\delta}^A - \cdots\right) + \cdots \\ = Tq^A q^B + T_\alpha(q^A\hat{\mu}_\alpha^B - q^B\hat{\mu}_\alpha^A) &+ T_{\alpha\beta}\left(\frac{1}{3}q^A\widehat{\Theta}_{\alpha\beta}^B - \hat{\mu}_\alpha^A\hat{\mu}_\beta^B + \frac{1}{3}q^B\widehat{\Theta}_{\alpha\beta}^A\right) + \cdots\end{aligned} \tag{2.2.5}$$

this expression is an operator, therefore if we require the electrostatic interaction potential then we must take the expectation value of $\mathcal{H}'$.

If we were to have N interacting molecules instead of two, the interaction energy can be generalized by summing these contributions pairwise given that the Coulombic interactions is strictly additive.

2.2.1 Perturbation theory for long-range interactions.

If the molecules A and B are far enough apart the multipolar expansion (2.2.5) will be valid and the interaction energy small. In this situation perturbation theory is a valid approach to solve the eigenvalue equation of the Hamiltonian. Let's consider a set of electrons that are identified as belonging to molecule A. These electrons may be described by a wavefunction Ψ_m^A and a Hamiltonian $\mathcal{H}_A$ can be defined in terms of these electrons. The same can be stated for molecule B, with a wavefunction Ψ_m^B describing its electrons and a Hamiltonian $\mathcal{H}_B$ defined according to this set of electrons. The Hamiltonian for the two molecules, including the perturbative Hamiltonian $\mathcal{H}'$, can be written as:

$$\mathcal{H} = \mathcal{H}_A + \mathcal{H}_B + \mathcal{H}' = \mathcal{H}_0 + \mathcal{H}' \tag{2.2.6}$$

The unperturbed Hamiltonian for the combined system, $\mathcal{H}_0$, verifies the Symmetrisation Postulate of Quantum Mechanics: the exchange of any two identical particles of the system preserves the correct symmetry. Thus, the unperturbed states can be given as the product functions $\Psi_m^A \Psi_n^B$, which can be simplified as $|mn\rangle$. We have, then, the energy eigenstates:

$$\mathcal{H}_0|mn\rangle = (\mathcal{H}_A + \mathcal{H}_B)|mn\rangle = (W_m^A + W_n^B)|mn\rangle = W_{mn}^0|mn\rangle \tag{2.2.7}$$

where $\mathcal{H}_A|m\rangle = W_m^A|m\rangle$ and $\mathcal{H}_B|n\rangle = W_n^B|n\rangle$ are the energy eigenstates of the isolated A and B molecules, respectively, and $|mn\rangle = |m_A n_B\rangle = |m_A\rangle \otimes |n_B\rangle$ is the product of their state bases.

For a simpler argument let's assume that the interacting molecules have a closed shell electronic structure, such that their ground states are non-degenerate. The energy of the ground state of the two interacting molecules in second order perturbation theory [2] is, therefore:

$$\begin{aligned} W_{00} &= W_{00}^0 + W_{00}^{(1)} + W_{00}^{(2)} \\ &= W_{00}^0 + \langle 00|\mathcal{H}'|00\rangle - \sum_{m,n\neq 0} \frac{\langle 00|\mathcal{H}'|mn\rangle\langle mn|\mathcal{H}'|00\rangle}{W_{mn}^0 - W_{00}^0} \end{aligned} \tag{2.2.8}$$

In most cases it suffices to truncate the perturbation series in its second order, but in certain systems the third order contribution may be relevant. For example, these third order terms account for the three-body dispersive non-additive effects (Axilrod–Teller–Muto potential) [1].

2.2.2 Electrostatic interaction.

The zeroth order contribution to the energy, W_{00}^0, is a constant value which represents the sum of the energies of the isolated molecules A and B and may be suppressed by taking an

appropriate origin for the energy. In the ground state of the unperturbed system the first order contribution, $W_{00}^{(1)}$, is the expected value of the electrostatic Hamiltonian, $\mathcal{H}'$.

If we go back to the multipolar expansion series (2.2.5), the interaction energy becomes:

$$\begin{aligned} U_{es} &= \langle 00|\mathcal{H}'|00\rangle = \langle \mathcal{H}' \rangle_{00} \\ &= Tq^A q^B + T_\alpha (q^A \langle \hat{\mu}_\alpha^B \rangle_0 - q^B \langle \hat{\mu}_\alpha^A \rangle_0) \\ &+ T_{\alpha\beta}\left(\frac{1}{3} q^A \langle \widehat{\Theta}_{\alpha\beta}^B \rangle_0 - \langle \hat{\mu}_\alpha^A \rangle_0 \langle \hat{\mu}_\alpha^B \rangle_0 + \frac{1}{3} q^B \langle \widehat{\Theta}_{\alpha\beta}^A \rangle_0 \right) + \cdots \end{aligned} \tag{2.2.9}$$

the expected values of the molecular operator [6] are calculated by choosing an appropriate closure relationship in the position state basis set of each molecule. Altogether, it can be concluded that both the multipolar expansion and the non-expanded expression (2.1.3) represent the electrostatic interaction between two molecules.

For two neutral species the electrostatic interaction energy is written as the sum of the dipole-dipole term, dipole-quadrupole, quadrupole-quadrupole, etc.:

$$\begin{aligned} U_{es} &= -T_{\alpha\beta}\mu_\alpha^A \mu_\beta^B - \frac{1}{3} T_{\alpha\beta\gamma}\left(\mu_\alpha^A \Theta_{\beta\gamma}^B - \Theta_{\alpha\beta}^A \mu_\gamma^B\right) \\ &- T_{\alpha\beta\gamma\delta}\left(\frac{1}{15}\mu_\alpha^A \Omega_{\beta\gamma\delta}^B - \frac{1}{9}\Theta_{\alpha\beta}^A \Theta_{\gamma\delta}^B + \frac{1}{15}\Omega_{\alpha\beta\gamma}^B \mu_\delta^B\right) + \cdots \end{aligned} \tag{2.2.10}$$

In order to illustrate the electrostatic energy and obtain a treatable expression, let's consider the simplest case of two neutral molecules such that only the dipole-dipole interaction contributes to the potential energy. Therefore:

$$U_{\mu\mu} = -T_{\alpha\beta}\left(\mu_\alpha^A \mu_\beta^B\right) = \frac{R^2 \mu^A \mu^B - 3\left(\mu^A \cdot \vec{R}\right)\left(\mu^B \cdot \vec{R}\right)}{4\pi\varepsilon_0 R^5}$$

$$= -\frac{\mu^A \mu^B}{4\pi\varepsilon_0 R^3}(2\cos\theta_A \cos\theta_B - \sin\theta_A \sin\theta_B \cos\varphi) = -\frac{\mu^A \mu^B}{4\pi\varepsilon_0 R^3}\,\Upsilon(\theta_A, \theta_B, \varphi) \tag{2.2.11}$$

As was done in section 1.3, and taking **Fig. 1.3** as reference, the global Z axis is set along $\vec{R}$, with the origin at molecule A. The direction of the dipoles μ^A and μ^B is specified by the polar angles θ_A, φ_A and θ_B, φ_B. By choosing the X axis to coincide with the local x_A axis of the molecule A, $X \equiv x_A$, then the polar angles become related, $\varphi = \varphi_A - \varphi_B$.

Furthermore, it is clear that the most energetically favourable orientation would have $\Upsilon(0, 0, 0)$, representing a *head-tail* configuration, and in this case the angular factor would be -2. The most unfavourable orientations would have $\Upsilon(\pi, 0, 0)$ and $\Upsilon(0, \pi, 0)$ or *head-head*

[6] In order to simplify the bra-ket notation, the matrix elements are expressed as: $\langle 0_A 0_B|\hat{A}|0_A 0_B\rangle = \langle 00|\hat{A}|00\rangle = \langle \hat{A} \rangle_{00}$

configuration, with an angular factor $+2$. Either $\Upsilon\left(-\frac{\pi}{2},\frac{\pi}{2},0\right)$, antiparallel, or $\Upsilon\left(\frac{\pi}{2},\frac{\pi}{2},\pi\right)$, parallel, would be attractive for dipolar molecules, which would give an angular factor -1.

2.2.3 Induction or polarization interaction.

The second order energy describes the induction and dispersion energies. This is appreciated when the second order term that appears in (2.2.7) is separated into three parts. The combination of excited and ground states for each molecule expresses the induction energy, whilst having both molecules in excited states refers to the dispersion energy:

$$W'' = U_{ind}^{A} + U_{ind}^{B} + U_{disp}$$

where:

$$U_{ind}^{A} = -\sum_{m\neq 0}\frac{\langle 00|\mathcal{H}'|m0\rangle\langle m0|\mathcal{H}'|00\rangle}{W_m^{\mathrm{A}} - W_0^{A}} \tag{2.2.12}$$

$$U_{ind}^{B} = -\sum_{n\neq 0}\frac{\langle 00|\mathcal{H}'|0n\rangle\langle 0n|\mathcal{H}'|00\rangle}{W_n^{\mathrm{B}} - W_0^{B}} \tag{2.2.13}$$

$$U_{disp} = -\sum_{m,n\neq 0}\frac{\langle 00|\mathcal{H}'|mn\rangle\langle mn|\mathcal{H}'|00\rangle}{W_m^{A} + W_n^{B} - W_0^{\mathrm{A}} - W_0^{\mathrm{B}}} \tag{2.2.14}$$

By means of the expansion (2.2.8) truncated at the second order term, the induction energy (2.2.13) becomes:

$$\begin{aligned} U_{ind}^{B} = -\sum_{n\neq 0}\frac{1}{W_n^{\mathrm{B}} - W_0^{B}}\langle 00\big|\left(Tq^{A}q^{B} + T_{\alpha}(q^{A}\hat{\mu}_{\alpha}^{B} - q^{B}\hat{\mu}_{\alpha}^{A}) - T_{\alpha\beta}\hat{\mu}_{\alpha}^{A}\hat{\mu}_{\beta}^{B} + \cdots\right)\big|0n\rangle \\ \times\langle 0n\big|\left(Tq^{A}q^{B} + T_{\alpha'}\left(q^{A}\hat{\mu}_{\alpha'}^{B} - q^{B}\hat{\mu}_{\alpha'}^{A}\right) - T_{\alpha'\beta'}\hat{\mu}_{\alpha'}^{A}\hat{\mu}_{\beta'}^{B} + \cdots\right)\big|00\rangle \end{aligned} \tag{2.2.15}$$

the matrix elements of the first term vanish because q^{B} is just a constant and any molecular excited state would be orthogonal to the molecule's ground state. Considering the orthonormality relationships in the state's basis of molecule A, the implied integration over its coordinates is performed. This gives:

$$\begin{aligned} U_{ind}^{B} &= -\frac{1}{2}\left(q^{A}T_{\alpha} - T_{\alpha\beta}\hat{\mu}_{\alpha}^{A} + \cdots\right)\alpha_{\alpha\alpha'}^{B}\left(q^{A}T_{\alpha'} - T_{\alpha'\beta'}\hat{\mu}_{\alpha'}^{A} + \cdots\right) - \cdots \\ &= -\frac{1}{2}\,F_{\alpha}^{A}\alpha_{\alpha\alpha'}^{B}F_{\alpha'}^{A} - \cdots \end{aligned} \tag{2.2.16}$$

the expression F_{α}^{A} is the electric field components created by molecule A at the position of molecule B and the quantum mechanical expression is identified as being the components of the electric dipole-dipole polarizability tensor of molecule B. The dipolar polarizability gives

the measure by which an external and constant electric field would induce a dipolar momentum in a given molecule. This magnitude can be calculated through the following expression [1]:

$$\alpha^B_{\alpha\alpha'} = \sum_{n\neq 0}\sum_{n\neq 0} \frac{\langle 0|\hat{\mu}^B_\alpha|n\rangle_B\langle n|\hat{\mu}^B_{\alpha'}|0\rangle_B + \langle 0|\hat{\mu}^B_{\alpha'}|n\rangle_B\langle n|\hat{\mu}^B_\alpha|0\rangle_B}{W^{\mathrm{B}}_n - W^B_0} \tag{2.2.17}$$

If the static dipole-quadrupole and quadrupole-quadrupole polarizabilities of the molecule B, $A^B_{\alpha,\alpha'\beta'}$ and $C^B_{\alpha\beta,\alpha'\beta'}$ respectively, are included in the induction energy (2.2.16) as was done for the electrostatic energy (2.2.10), then it reads:

$$U^B_{ind} = -\frac{1}{2}F^A_\alpha\alpha^B_{\alpha\alpha'}F^A_{\alpha'} - \frac{1}{3}F^A_\alpha A^B_{\alpha,\alpha'\beta'}F^A_{\alpha'\beta'} - \frac{1}{6}F^A_{\alpha\beta}C^B_{\alpha\beta,\alpha'\beta'}F^A_{\alpha'\beta'} - \cdots \tag{2.2.18}$$

In some situations it is necessary to consider non-linear polarizability effects or hyperpolarizabilities, which are terms beyond the second-order perturbation theory.

To clarify the form of the induction interaction, let us consider the interaction of an ion A, and a noble gas atom B, both being in their ground states and having a closed electronic shell. This is the configuration that will be treated in section 4.2. Due to the symmetry of closed shell atoms their electric dipolar polarizabilities are isotropic. The polarizability tensor is diagonal for such a case, $\alpha^A_{\alpha\gamma} = \alpha^A\delta_{\alpha\gamma}$ and $\alpha^B_{\beta\delta} = \alpha^B\delta_{\beta\delta}$, and the electric field produced by the ion would be $F_z = -q/4\pi\varepsilon_0 Z^2$ along the Z axis. The induction energy created by the ion on the atom would be $U^B_{ind} = -q^2\alpha^B/4\pi\varepsilon_0 Z^4$. From this we can gather that the electric field goes with R^{-2} and the induction energy goes as R^{-4}. For an electrically neutral but dipolar molecule ($q^A = 0$, $\mu^A \neq 0$), the electric field goes with R^{-3} and the induction energy goes as R^{-6}. In each of these cases the induction energy is always attractive.

It is worthwhile pointing out that the electric field F^A_α for a molecule B surrounded by many molecules will be the vector sum of the electric fields generated by the A molecules. In such a situation, the induction energy cannot be described by simple pairwise addition and therefore it displays a non-additive character.

2.2.4 Dispersion interaction.

Returning to equation (2.2.15) and considering only the first non-zero contribution in $\mathcal{H}'$ for electrically neutral molecules, the dipole-dipole term, the expression becomes:

$$U^{(6)}_{disp} = -\sum_{\mathrm{m,n}\neq 0} \frac{\langle 00|\hat{\mu}^A_\alpha T_{\alpha\beta}\hat{\mu}^B_\beta|\mathrm{mn}\rangle\langle \mathrm{mn}|\hat{\mu}^A_\gamma T_{\gamma\delta}\hat{\mu}^B_\delta|00\rangle}{W^A_m + W^B_n - W^{\mathrm{A}}_0 - W^{\mathrm{B}}_0}$$

$$= -T_{\alpha\beta}T_{\gamma\delta}\sum_{\mathrm{m,n}\neq 0} \frac{\langle 0|\hat{\mu}^A_\alpha|m\rangle\langle 0|\hat{\mu}^B_\beta|n\rangle\langle m|\hat{\mu}^A_\gamma|0\rangle\langle n|\hat{\mu}^B_\delta|0\rangle}{W^A_{m0} + W^B_{n0}} \tag{2.2.19}$$

where $W_{m0}^{A} = W_{m}^{A} - W_{0}^{\mathrm{A}}$ and $W_{n0}^{B} = W_{n}^{B} - W_{0}^{\mathrm{B}}$. Although the numerator of this expression can be factorized into terms referring to molecule A and terms referring to molecule B, the denominator cannot.

One way to deal with this difficulty is due to London (1930), who rewrote (2.2.19) as:

$$U_{disp}^{(6)} = -T_{\alpha\beta}T_{\gamma\delta}\sum_{\mathrm{m,n}\neq 0}\frac{W_{m0}^{A}W_{n0}^{B}}{W_{m0}^{A}+W_{n0}^{B}}\frac{\langle 0|\hat{\mu}_{\alpha}^{A}|m\rangle\langle m|\hat{\mu}_{\gamma}^{A}|0\rangle}{W_{m0}^{A}}\frac{\langle 0|\hat{\mu}_{\beta}^{B}|n\rangle\langle n|\hat{\mu}_{\delta}^{B}|0\rangle}{W_{n0}^{B}} \qquad (2.2.20)$$

The terms $W_{m0}^{A}W_{n0}^{B}/(W_{m0}^{A}+W_{n0}^{B})$ do not allow factoring out the product of static dipolar electric polarizability components $\alpha_{\alpha\gamma}^{A}$ and $\alpha_{\beta\delta}^{B}$ (2.2.17). A first approach is to express this is in terms of the averaged excitation energies U_A and U_B, *id est*, to follow the Unsöld approximation:

$$U_{disp}^{(6)} \approx -\frac{U_A U_B}{4(U_A+U_B)}T_{\alpha\beta}T_{\gamma\delta}\alpha_{\alpha\gamma}^{B}\alpha_{\beta\delta}^{B} \qquad (2.2.21)$$

Considering again the simple case of isotropic polarizabilities, $\alpha_{\alpha\gamma}^{A} = \alpha^{A}\delta_{\alpha\gamma}$ and $\alpha_{\beta\delta}^{B} = \alpha^{B}\delta_{\beta\delta}$, and taking into the account the form of the interaction tensors (2.2.3), the following expression is obtained:

$$U_{disp}^{(6)} \approx -\frac{U_A U_B}{4(U_A+U_B)}T_{\alpha\alpha}T_{\alpha\alpha}\alpha^{A}\alpha^{B} = -\frac{3U_A U_B}{2(U_A+U_B)}\frac{\alpha^{A}\alpha^{B}}{(4\pi\varepsilon_0)^2 R^6} = -\frac{C_6}{R^6} \qquad (2.2.22)$$

this is the well-known London formula for the dispersion energy between two atoms and it can also be used for molecules when it gives the dispersion interaction averaged over relative orientations of the two molecules. This expression is not often employed to estimate the dispersion energy due to the difficulty of estimating the average excitation energies, but upper and lower limits may be obtained by substituting U_A and U_B by either the first excitation energies or the ionization potentials for A and B.

A mathematically exact form of the dispersion energy is based on the work of Casimir and Polder (1948), which employs the following mathematical identity:

$$\frac{1}{A+B} = \frac{2}{\pi}\int_0^{\infty}\frac{AB}{(A^2+\vartheta^2)(b^2+\vartheta^2)}d\vartheta \qquad (2.2.23)$$

which is valid for A, B positive and can be established by a contour integration on the complex plane. Applying this formula to the energy denominator in (2.2.20), where $W_{m0}^{A} + W_{n0}^{B} = \hbar(\omega_m^A + \omega_n^B)$, we get:

$$U_{disp}^{(6)} = -\frac{2\hbar}{\pi}T_{\alpha\beta}T_{\gamma\delta}\int_0^{\infty}\sum_{m\neq 0}\frac{\omega_m^A\langle 0|\hat{\mu}_{\alpha}^{A}|m\rangle\langle m|\hat{\mu}_{\gamma}^{A}|0\rangle}{\hbar((\omega_m^A)^2+\vartheta^2)}\sum_{n\neq 0}\frac{\omega_n^B\langle 0|\hat{\mu}_{\beta}^{B}|n\rangle\langle n|\hat{\mu}_{\delta}^{B}|0\rangle}{\hbar((\omega_n^B)^2+\vartheta^2)}\,d\vartheta \qquad (2.2.24)$$

here we can look at equation (2.2.17) to recognize the summations over states as being the dynamic polarizabilities of A and B at the imaginary frequency $i\vartheta$ [1], and expression (2.2.14) can be written as:

$$U_{disp}^{(6)} = -\frac{\hbar}{2\pi} T_{\alpha\beta} T_{\gamma\delta} \int_0^\infty \alpha_{\alpha\gamma}^B(i\vartheta)\alpha_{\beta\delta}^B(i\vartheta)d\vartheta \tag{2.2.25}$$

The dynamic polarizability expresses the response of the molecule to an external electric field which is sinusoidally dependent with time. This magnitude is closely tied to atomic and molecular spectroscopy. The dynamic polarizability at imaginary frequencies $\alpha_{\alpha\gamma}^B(i\vartheta)$ does not have an easy physical interpretation but its mathematical properties are sufficiently regular and the integral (2.2.25) can be solved numerically.

Similarly to the London-Unsöld treatment, the dispersion energy $U_{disp}^{(6)}$ will now become:

$$U_{disp}^{(6)} = -\frac{3\hbar}{(4\varepsilon_0)^2\pi^3 R^6} \int_0^\infty \alpha^A(i\vartheta)\alpha^B(i\vartheta)d\vartheta = -\frac{C_6}{R^6} \tag{2.2.26}$$

By including higher order components in the expression (2.2.14), terms depending on dynamic polarizabilities for dipole-quadrupole, quadrupole-quadrupole, dipole-octupole, etc. appear under the integral. For centrosymmetric atoms this treatment simplifies and leads to:

$$U_{disp} = -\frac{C_6}{R^6} - \frac{C_8}{R^8} - \frac{C_{10}}{R^{10}} - \cdots \tag{2.2.27}$$

where:

$$C_6 = C_{\mu,\mu}^{AB} \qquad C_8 = C_{\mu,\Theta}^{AB} + C_{\Theta,\mu}^{AB} \qquad C_{10} = C_{\Theta,\Theta}^{AB} + C_{\mu,\Omega}^{AB} + C_{\Omega,\mu}^{AB} \tag{2.2.28}$$

Following Casimir and Polder's method, the different C_n coefficients for even indexes n can be obtained from the corresponding integrals [7]. For instance, the coefficient $C_{\mu,\Theta}^{AB}$ is $\frac{15\hbar}{2(4\varepsilon_0)^2\pi^3 R^8}\int_0^\infty \alpha^A(i\vartheta)A^B(i\vartheta)d\vartheta$.

Note as well that for more complicated molecular interactions, the C_n coefficients will depend on the relative orientations of the molecules. The higher order contributions are to be included in accurate calculations, however, as we shall see, they are reduced by damping effects.

2.3 Short-range molecular interactions

So far we've been ignoring exchange effects associated with the overlapping of anti-symmetrized wave functions. The reason behind this simplification is that at large distances these contributions tend to zero and only the attractive electrostatic terms raised by the

molecular electronic wave functions prevail. In the case of short-range interactions the exchange-repulsion effects play a major role and the quantum mechanical treatment with standard perturbation theory fails in this situation. For an introductory study such as the present work, going into a lengthy discussion on short-range interactions would be impractical and, therefore, the simplest treatment is presented to explore these complications.

2.3.1 Perturbation theory for short-range interactions.

By taking a look at the usual Rayleigh-Ritz perturbation theory [2], the limitations of perturbative models at short range are immediately apparent:

- There isn't an unambiguous definition up to the order of the perturbation expansion given that the unperturbed and perturbed terms of the Hamiltonian are non-invariant with respect to electron permutation.
- The Hamiltonian eigenstates must be anti-symmetrized, hence, even if the states $|m_A\rangle|n_B\rangle$ are orthogonal, the anti-symmetrized products $|m_A n_B\rangle$ are not. A set of orthonormal eigenstates cannot be formed.

There are many perturbative methods [1] proposed to deal with the anti-symmetry of the unperturbed states, but the first order energy is the same in all of them: basically it is the difference between the expected value of the system Hamiltonian $\mathcal{H}$ in the anti-symmetrized product state $|0_A 0_B\rangle$ and the zeroth order energy of the non-interactive system, which is a unique constant and disappears through proper choice of origin of the energy coordinates:

$$E_{00}^{(1)} = \langle \mathcal{H} \rangle_{00} - (W_0^{\mathrm{A}} + W_0^{\mathrm{B}}) \tag{2.3.1}$$

2.3.2 Electrostatic interaction: penetration effects.

The electrostatic energy described by the relation (2.1.3) can be made to converge at any distance but fails at short distances when the molecular charge distributions overlap. The converged result is in error by an amount known as *penetration energy*.

Let's take the situation of a proton interacting with a hydrogen-like atom of nuclear charge Z to simply illustrate this behaviour. The ground state wavefunction of the atom is $\varphi_{1s}(R) = \sqrt{Z^3/\pi}\, e^{-ZR}$, the associated charge distribution will be $\rho(R) = -e|\, \varphi_{1s}(R)|^2 = -e(Z^3/\pi)e^{-2ZR}$. The electrostatic potential $V(R)$ generated at a distance R from the atom's nucleus by the electric charge distribution is obtained by solving Poisson's equation $\nabla^2 V = -\rho(R)/\varepsilon_0 = 4Z^3 e^{-2ZR}$, where $4\pi\varepsilon_0 = 1$ in atomic units. The charge density is spherically symmetric and so is the potential, thus:

$$V(R) = -\frac{1}{R} + \left(Z + \frac{1}{R}\right) e^{-2ZR} = -\frac{1}{R}[1 - e^{-2ZR}(1 + RZ)] = -\frac{1}{R} f_1(2ZR) \tag{2.3.2}$$

The function $f_1(2ZR)$ is known as the *damping function*, its value is 1 at long range and tends to zero at short range as to suppress the singularity of the electric monopole term (the charge). The exponential term describes the penetration correction to the potential at short-range that arises from the finite extent of the charge distribution. The general case must include the higher-order electric multipole terms and all R^{-n} singularities are cancelled out from the complete penetration correction, leaving only the term Z/R from the electron-nuclei interaction. The dispersion and induction terms are also accompanied by singularities of this kind and are normally treated by means of their corresponding damping functions.

2.3.3 Exchange and repulsion interactions.

If the anti-symmetrisation of a two-molecule system's wavefunction is performed new contributions to the electrostatic energy appear [1]. These are the exchange and repulsion terms. From the perturbative treatment a simple agreement about the dependency with distance of the energy of exchange and repulsion can be reached: it changes exponentially with the separation distance R. An accurate representation would be a function of the form:

$$U_{er} = Ke^{-b(R-R_0)} \tag{2.3.3}$$

where K is an arbitrary fixed constant (for instance: $U_{er} = K$ when $R = R_0$), b is a parameter that accounts for the range of the energy of exchange and repulsion and typically varies around $2 - 4$ Å^{-1}, it is also known as a Born-Mayer parameter, and R_0 depends on the size and structure of the interacting molecules concerned.

2.3.4 Induction and dispersion interactions: damping effects.

From the symmetry-adapted perturbative theory calculations at short range it is clear that the second-order contributions stay finite when the separation R between molecules goes to zero. The only singularity arises from the electrostatic terms associated to the repulsion between the nuclei of the system's atoms. With this in mind and considering the expression (2.2.26), let's multiply each term by the corresponding damping function to resolve the singularities:

$$U_{disp} = -f_6(R)\frac{C_6}{R^6} - f_8(R)\frac{C_8}{R^8} - f_{10}(R)\frac{C_{10}}{R^{10}} - \cdots \tag{2.3.4}$$

Each damping function $f_n(R)$ must suppress the corresponding R^{-n} singularity so it should tend to zero or to a constant with the behaviour R^n when $R \to 0$. In the literature there are several functional forms of these damping functions [1], in the next chapter we introduce one of the most popular: the Tang-Toennies damping function.

In the simplest case, the interaction between a closed-shell ion and an atom, the induction energy's leading term in the multipole expansion at short distances behaves according to R^{-4}, while for neutral polar molecules it is proportional to R^{-6}. At short ranges, these terms must be multiplied as well by the corresponding damping functions.

3 Interaction potential models

The main goal of this chapter is to present some of the historical potential models, the Lennard-Jones and Born-Mayer potentials, as well as the more realistic Tang-Toennies and Pirani potentials. These treatable mathematical functions will be employed in the fourth chapter to illustrate and compare their behaviour computationally in atomic systems.

3.1 The Lennard-Jones potential

It was first introduced in 1906 by Mie and later adopted by Lennard-Jones, and it consists of a repulsive term C_n/R^n and attractive term $-C_m/R^m$ with $n > m$. After London's work on the dispersion forces the values $m = 6$ and typically $n = 12$ were chosen. The LJ potential is:

$$U_{LJ}(R) = 4\varepsilon\left[\left(\frac{\sigma}{R}\right)^{12} - \left(\frac{\sigma}{R}\right)^{6}\right] = \varepsilon\left[\left(\frac{R_e}{R}\right)^{12} - 2\left(\frac{R_e}{R}\right)^{6}\right] \tag{3.1.1}$$

where ε represents the depth of the potential well, R_e being the position of the equilibrium position (the minimum position such that $U_{LJ}(R_e) = -\varepsilon$), $\sigma = 2^{-1/6}R_e$ is the position where the repulsive branch crosses zero. Therefore, the potential depends on two parameters, R_e or σ and ε, which can be adjusted to experimental data and/or *ab initio* calculations. The attractive term is the leading term in the R^{-1} expansion of the dispersion energy. The repulsive term has no theoretical justification, beyond its steep repulsive form, given that it should be of exponential form.

From a mathematical standpoint this model potential is a particular case of a family of analytical functions, or Mie potentials, sometimes called generalized LJ potentials, which are characterized by a minimum of energy in R_e independent of the parameters m, n, where $n > m$, and an acceptable asymptotic behaviour for $R \to \infty$. These potentials have the form:

$$U_{LJ}(n, m, R) = \varepsilon\left[\frac{m}{n-m}\left(\frac{R_e}{R}\right)^{n} - \frac{n}{n-m}\left(\frac{R_e}{R}\right)^{m}\right] \tag{3.1.2}$$

3.2 The Born-Mayer potential

Born and Mayer suggested in 1932 to replace the repulsive term of the LJ potential by an exponentially decreasing function, which, combined with the London expression for the dispersion contribution, gave rise to the 'exp-6' potential:

$$U_{exp-6}(R) = U_{BM}(R) + U_{disp}^{(6)} = Ae^{-bR} - \frac{C}{R^6} \tag{3.2.1}$$

Both the exp-6 potential and the Buckingham-Corner potential, which has a R^{-8} dispersion term as well, are unsuitable for some calculations but are physically acceptable. The reason is that the exponential part tends to the constant A as the separation decreases, yet it remains finite when $R = 0$, so the dispersive term becomes dominant at very short-range and the potential has an incorrect behaviour, leading to $U_{exp-6}(R \to 0) \to -\infty$.

Alas, in the time of its inception the exponential part was computationally inconvenient so the LJ potential was preferred although it too has obvious deficiencies.

3.3 The Tang-Toennies potential

An accurate description of the van der Waals potentials is provided by the Tang-Toennies potential introduced in 1984 [3], which has recently been shown to be a generalized form of the Heitler-London theory, with a five-parameter analytical expression: the first three dispersion coefficients C_6, C_8 and C_{10} and the parameters A and b of the BM repulsion potential.

In this model, the short-range repulsive BM potential is added to a damped dispersion:

$$U_{TT}(R) = Ae^{-bR} - \sum_{k=3}^{K} f_{2k}(bR)\frac{C_{2k}}{R^{2k}} \tag{3.3.1}$$

For most rare gas systems the C_{2k} coefficients can be obtained theoretically with high accuracy. Note that the BM range parameter b is the only parameter in the damping functions $f_{2k}(bR)$, understandable when considering that the damping of the dispersion potential is a consequence of the wavefunction overlapping.

These damping functions are incomplete gamma functions:

$$f_{2k}(bR) = 1 - \frac{\gamma(2\mathrm{k}+1, \mathrm{bR})}{2k!} = 1 - e^{-bR}\sum_{n=0}^{2k}\frac{[bR]^n}{n!} \tag{3.3.2}$$

where we may verify that $f_{2k}(R \to 0) \to 0$, where $\gamma(2\mathrm{k}+1, \mathrm{bR})$ has a R^{2k+1} behaviour for small R, and $f_{2k}(R \to \infty) \to 1$, thus correcting the improper behaviour of the dispersion

contribution. This can be proven by taking a look at some inequalities that follow easily from the incomplete gamma function $\gamma(2k+1, bR) = \int_0^{bR} t^{2k} e^{-t} dt$ [5]. If the boundary $0 \leq t \leq bR$ is applied, then $t^{2k} e^{-bR} \leq t^{2k} e^{-t} \leq t^{2k}$ and $\gamma(2k+1, bR)$ is bounded in the following fashion:

$$e^{-bR} \frac{(bR)^{2k+1}}{2k+1} \leq \gamma(2k+1, bR) \leq \frac{(bR)^{2k+1}}{2k+1} \tag{3.3.3}$$

where $\gamma(2k+1, bR) \sim bR^{2k+1}/(2k+1)$ as $R \to 0$.

These damping functions acting on the dispersive terms R^{-6}, R^{-8} and R^{-10} are shown in **Fig. 3.1** for the He-He dimer employing the BM parameter $b = 1.335$ Å^{-1} that corresponds to a He-He interaction.

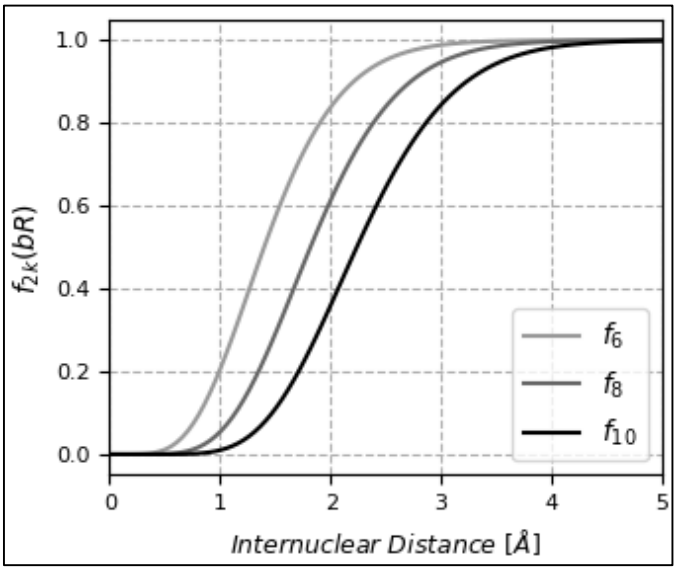

Fig. 3.1. Tang-Toennies damping functions of orders 6, 8 and 10 for the He dimer.

As the order of the dispersive term goes up the distance at which the damping function becomes effective is greater, thus the behaviour $U_{TT}(R \to 0) \to \infty$ is attenuated by the lower order terms and truncating the series at 2k=10 is usually sufficient to correct the dispersive potential in the van der Waals region. However, one may notice that the TT damping functions over-dampen the dispersive term U_{disp} at $R \to 0$.

Overall, the Tang-Toennis model uniquely determines the BM parameters A and b when a given set of well parameters, R_e and ϵ, are chosen. Even though up to eight terms are necessary for convergence, dropping the higher order terms and keeping those associated with the damping functions f_6, f_8 and f_{10} introduces only a small error that can be corrected by the adjustment of A and b near the minimum of the potential.

3.4 The Pirani potential

It is an empirical potential model with just three parameters that are initially adjusted from high resolution experimental measurements of the effective cross-sections for collision of molecular beams of rare gases [4]. It is most commonly known as Improved Lennard-Jones potential. The Pirani potential eliminates most of the short and middle-range inadequacies of

the LJ model. The mathematical expression is derived from the Mie potential (3.1.2) and takes the form:

$$U_{ILJ}(\mathrm{R}) = \epsilon\left[\frac{m}{n(R)-m}\left(\frac{R_e}{R}\right)^{n(R)} - \frac{n(R)}{n(R)-m}\left(\frac{R_e}{R}\right)^{m}\right] \tag{3.4.1}$$

where, as before, ϵ and R_e represent the depth of the potential well and its location. The first term describes the repulsion and the second one represent the long-range attraction. For all neutral-neutral systems the value $m = 6$ is assumed, while for ion-neutral interactions $m = 4$ is chosen and $m = 1$ corresponds to ion-ion situations. The $n(R)$ term is found to be: $n(R) = \beta + 4\left(\frac{R}{R_e}\right)^2$. The β parameter is related to the hardness of the two interacting atoms and varies within a limited range following some regularities. Note also that $n(R \to 0) \to \beta$ and $n(R \to \infty) \to \infty$ and the expression (3.4.1) has a correct asymptotic behaviour.

The response of this potential is less repulsive than the LJ model, although it doesn't have an exponential repulsive term the short-range is less steep. It shows reasonable behaviour since the $n(R)$ dependence leads to a correct representation of the long-range attraction and attenuates the hardness of the repulsive wall as R decreases using only three parameters (ϵ, β, R_e). Moreover, the simply formulated and physically reliable Pirani model is particularly useful for molecular dynamics simulations of both neutral and ionic systems and it has been adapted for molecule-atom and molecule-molecule interactions by Pirani *et al* [4].

4 Interaction potentials between closed electron shell atoms

In this final chapter the potential models are presented and compared via simple Python scripts to obtain valid representations of the accurate interatomic van der Waals potentials for homogeneous rare gas dimers and for an atom-ion system, He-Li^+, as well as a three-body system He-He-Li^+.

4.1 Rare gas – rare gas interactions

The interatomic potentials are calculated for homogeneous pairs of rare gas atom, which have a closed shell electronic structure that simplifies the mathematical treatment.

4.1.1 Tang-Toennies potential

To study this potential model we make use of the parameters that Tang and Toennies fitted to *ab initio* calculations [3], which have been shown to be very precise.

In **Table I** the necessary dispersion coefficients as well as the Born-Mayer parameters A and b are presented along with the well minimum, R_e, and the well depth, ε, for each rare gas atom.

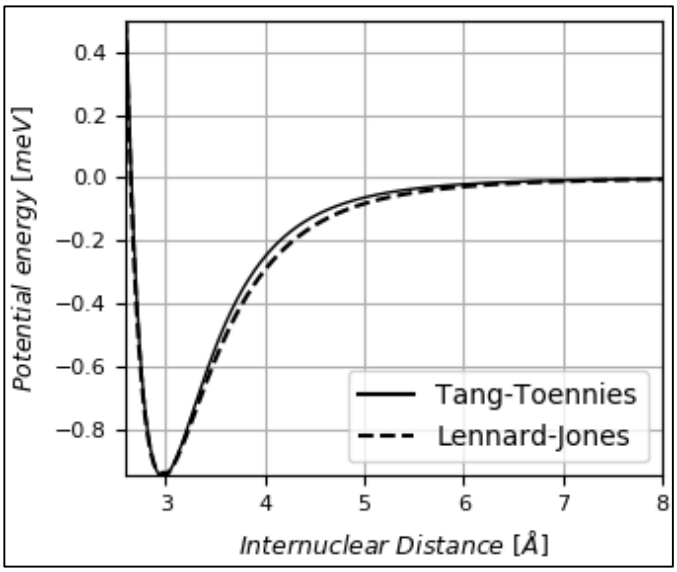

Fig. 4.1 TT and LJ potentials for the He dimer.

Firstly, let's consider the helium dimer interaction. We represent in **Fig. 4.1** the TT potential and, in order to show the differences with another potential model, a LJ potential whose parameters R_e and ε are set at the position and depth of the minimum energy of the TT potential is also represented. It is clearly seen that the TT potential has a stepper middle-range

Table I Parameters and equilibrium data for the homogeneous rare gas dimers.

$X-X$	$A\,(meV)$	$b\,(\text{Å})$	$C_6\,(meV\text{Å}^6)$	$C_8\,(meV\text{Å}^8)$	$C_{10}\,(meV\text{Å}^{10})$	$R_e\,(\text{Å})$	$\varepsilon\,(meV)$
He-He	$1.418 \cdot 10^6$	1.335	872.99	2360.95	8602.7	2.9739	0.9469
Ne-Ne	$5.429 \cdot 10^6$	1.301	3814.0	15116.1	71970.3	3.0904	3.6463
Ar-Ar	$2.036 \cdot 10^7$	1.705	38421	271567	2298738	3.7572	12.3539
Kr-Kr	$2.265 \cdot 10^7$	0.987	77439	700587	7286053	4.0111	17.3609
Xe-Xe	$2.59 \cdot 10^7$	0.89	170821	21443427	29041129	4.3657	24.3814
Rn-Rn	$1.514 \cdot 10^8$	0.965	251319	3222670	49994975	4.4768	34.2863

attractive region and, as seen from the close up, the repulsive short-range region is also slightly steeper. Naturally, both potential energy curves coincide at the well minimum, which corresponds to a value of $U\left(R_e = 2.9739\ \text{Å}\right) = -0.969\ meV$.

If we were to plot the rest of the noble gas PECs to further compare the behaviour of the TT potential model and the correspondingly fitted LJ potentials, the subtle differences apparent in the He dimer interaction potential become very great. This can be observed in **Fig. 4.2**, where all rare gas atom pairs, save for helium, are represented with their corresponding LJ PECs. In

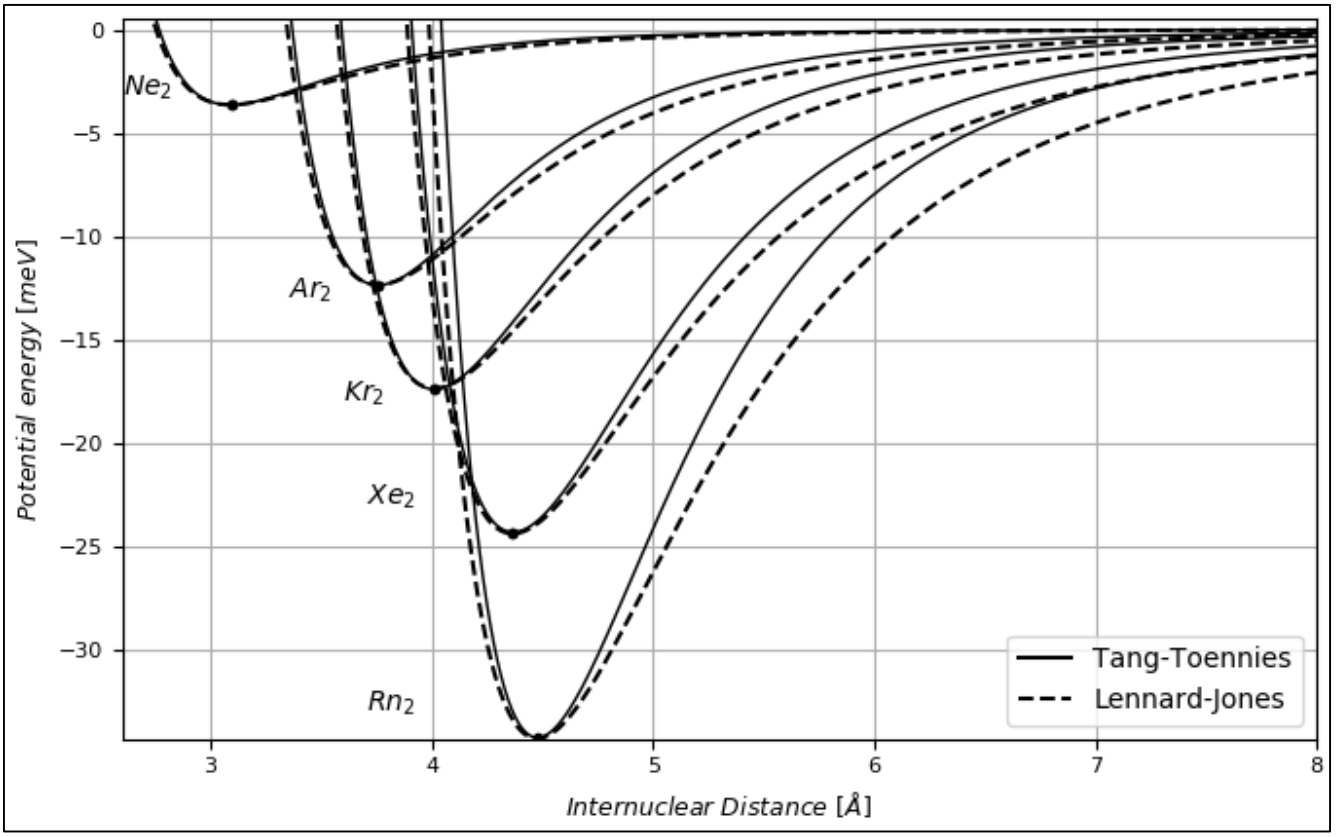

Fig. 4.2 TT and LJ potentials for the Ne, Ar, Kr, Xe and Rn dimers.

each case it is noticeable that the TT potential is steeper in both regions, repulsive and attractive, and the LJ potential merely has an adequate shape and a correct well minimum position and well depth but is altogether inaccurate as compared to the TT potential.

4.1.2 Pirani potential

To test the Pirani model (3.4.1), let's first consider a comparison with the LJ potential for the PEC of the He dimer. By using a $\beta = 9$ factor, in accordance with the analysis by Pirani *et al.* [4], as well as the values presented in **Table I.**

The resulting PEC seen in **Fig. 4.3** shows that the steepness of the response of the Pirani potential in the attractive and repulsive regions is greater, more so in the middle-range.

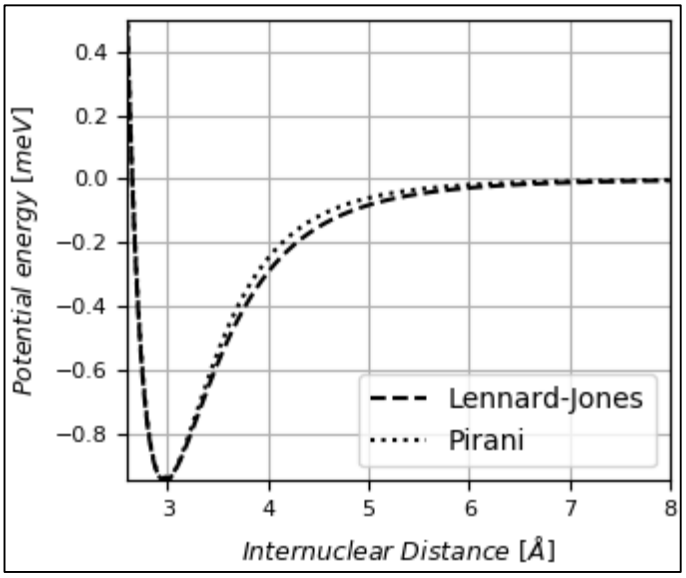

Fig. 4.3 ILJ and LJ potentials for the He dimer.

The PECs for the rest of the homogeneous rare gas dimers have also been obtained. As seen in **Fig. 4.4**, the response of the Pirani potential is very similar to the TT model with almost the same repulsive behaviour and also a slightly less attractive tendency in the

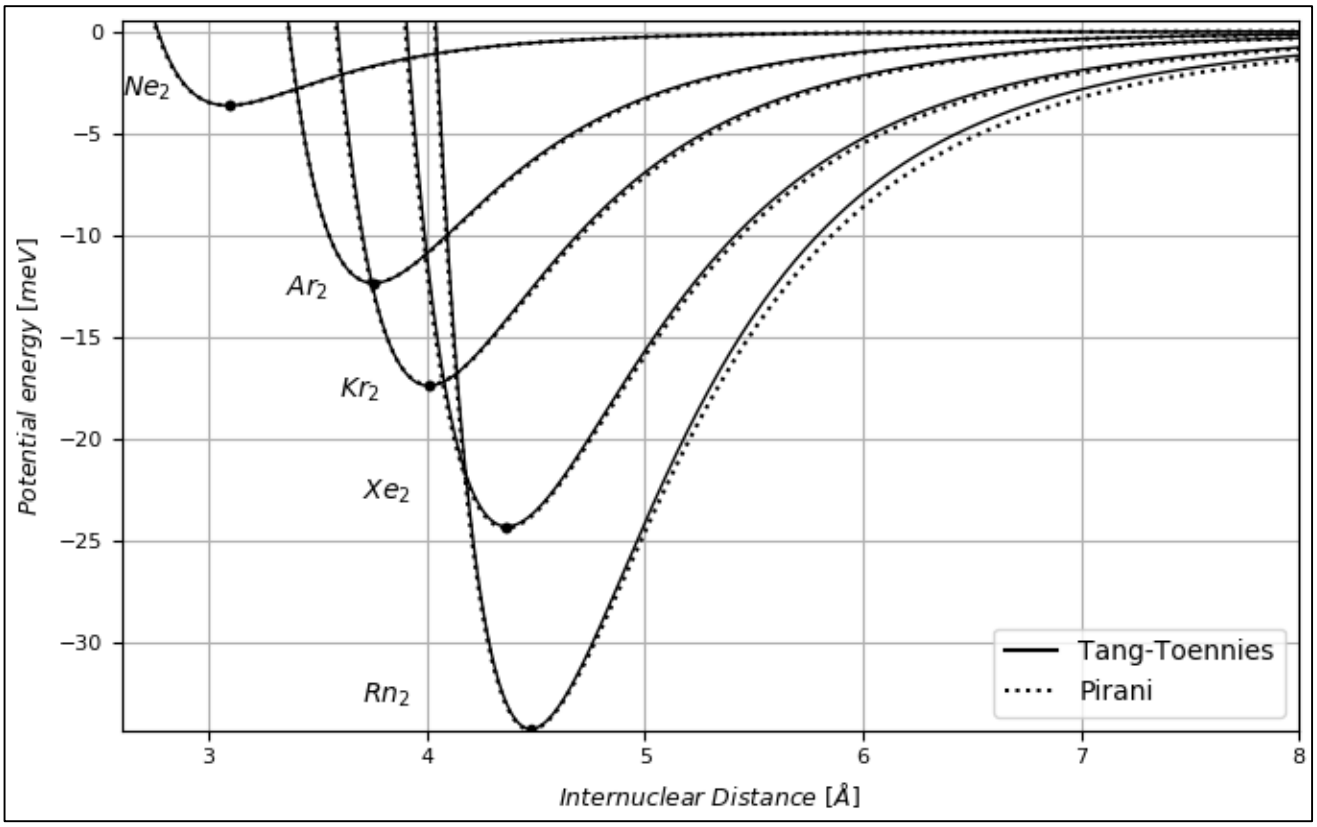

Fig. 4.4 Comparison of the ILJ and TT potentials for the Ne, Ar, Kr, Xe and Rn dimers.

middle and long-range. These PECs were obtained by employing the parameters from **Table I** and a different β factor of 10 and 11.5 for the Ar_2 and Rn_2 dimers respectively, as well as a β factor of 9.5 for the Ne_2, Kr_2 and Xe_2 dimers, while the He_2 dimer's factor is still set at 9. This deviation in choosing the β factor from the approach taken by Pirani *et al* provides a closer similarity of the Pirani PECs to the TT model while preserving the appropriate attractive and repulsive behaviour.

4.2 Atom-ion interactions for the He-Li^+ system

4.2.1 Soldán et al potential

This interatomic potential is employed for the interaction between a closed-shell metal ion and a rare gas atom, and is presented in the same way as Soldán *et al* [6]. It consists of a typical Born-Mayer potential for the repulsion term and the damped attractive induction and dispersion terms are expressed as a sum:

$$U_{Sol}(R) = Ae^{-bR} - \sum f_n(R)\frac{D_n}{R^n} \tag{3.5.1}$$

where the damping function is the same as in the Tang-Toennies potential. The coefficients D_n are related to the polarizabilities, hyperpolarizabilities and dispersion coefficients in the following manner:

$$D_4 = \frac{\alpha}{2}\ ;\ D_6 = \frac{A}{2} + C_6\ ;\ D_7 = \frac{B}{2}\ ;\ D_8 = \frac{C}{2} + \frac{\Upsilon}{24} + C_8 \tag{3.5.2}$$

here B and Υ are the dipole-dipole-quadrupole and second dipole hyperpolarizabilities, corresponding to the third and fourth order perturbation theory respectively. The expressions α, A and C are the static dipole-dipole, quadrupole-quadrupole and octupole-octupole polarizabilities.

The work carried out by Soldán *et al.* [6] will be reproduced, and to estimate how well they have fitted the parameters to first principle calculations, a Pirani potential is employed to represent the PEC of the same He-Li^+system. The parameters for the Soldán *et al.* potential (3.5.1) are those displayed in **Table II**. The dispersion coefficients D_n are calculated from the expression (3.5.2).

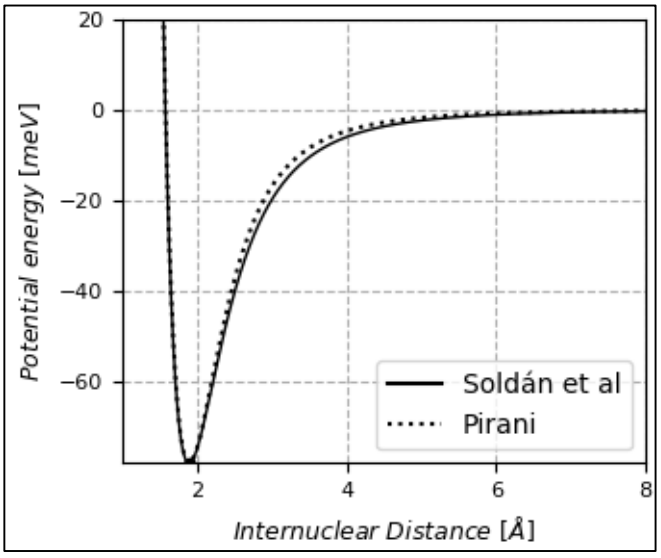

Fig. 4.5. Comparison between the Pirani and Soldán *et al.* potentials for the He-Li^+ system.

The calculations performed with the Soldán *et al.* model resulted in a different well minimum depth and position compared to the one calculated *ab initio* in their paper. The reason for this deviation is unknown, hence the Pirani potential is fitted to the well depth and position found with the Soldán *et al.* potential expression $U_{Sol}(R_e = 1.89\ \text{Å}) = -78.256\ meV$. A factor $\beta = 4.5$ and order $m = 4$ are the appropriate choices for this ion-atom setup.

These results are shown in **Fig. 4.5**, where it may be observed that the attractive middle region of the U_{Sol} potential is less pronounced than that of the Pirani model, and the repulsive region as well as the minimum energy of the interaction is described reasonably well by both potential models.

Table I Parameters for Soldán et al. potential.

$D_4(meV\text{Å}^4)$	$D_6\,(meV\text{Å}^6)$	$D_7\,(meV\text{Å}^7)$	$D_8\,(meV\text{Å}^8)$	$A\,(meV)$	$b\,(\text{Å}^{-1})$
1475.73	908.57	1158.34	1520.34	567852.57	4.826

4.2.2 Many-body system: He-He-Li$^+$

To study the PES of a three-body system as well as the many-body polarization correction mentioned in Sec. 1.2.2, a He-He-Li$^+$ trimer configuration as represented in **Fig. 4.6** is considered, and the approach taken by Liu *et al.* [9] is reproduced.

A first approximation to the PES of a three-body system can be expressed as the sum of three pairwise interactions:

$$V_{2B}(r_{12}, r_{13}, r_{23}) = V_{\text{Li}^+\text{He}}(r_{13}) + V_{\text{Li}^+\text{He}}(r_{23}) + V_{\text{HeHe}}(r_{12}) \qquad (4.3.1)$$

Each pairwise interaction can be calculated using the results already obtained in sections 4.1 and 4.2.1. We have chosen to use a Pirani potential for the He-He interaction and a Soldán *et al.* potential for the He-Li$^+$ interactions, employing the parameters displayed in **Table I** and **Table II.**

However, further considerations have to be taken into account given that the charged Li$^+$ ion will polarize the He atoms and an induced dipole will be created on both of them. These dipoles interact with each other, and this interaction is encompassed by a dipole-dipole potential energy term $V_{\mu\mu}$, the analytical expression was given in (2.2.11) and in the present case takes the form:

$$V_{\mu\mu} = \frac{\mu^{(1)}\mu^{(2)}}{r_{12}^3}(2\cos\phi_1\cos\phi_2 - \sin\phi_1\sin\phi_2) \qquad (4.3.2)$$

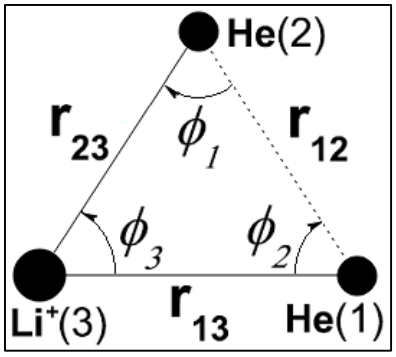

Fig. 4.6. Geometry of the He-He-Li$^+$ trimer system.

where $\mu^{(1)} = \alpha_{He}/r_{13}^2$ and $\mu^{(2)} = \alpha_{He}/r_{23}^2$ are the induced dipoles created by the electric charge of the ion. To include this dipole-dipole interaction potential in (4.3.1), it must be transformed through the appropriate trigonometric relations [7] to get rid of the angular dependency and leave it in terms of the interatomic distances r_{12}, r_{13} and r_{23}:

$$V_{\mu\mu} = -C_7\left(\frac{3r_{23}}{r_{13}^3 r_{12}^5} + \frac{3r_{12}}{4r_{23}^3 r_{12}^5} - \frac{1}{r_{23}^3 r_{13}^3 r_{12}} - \frac{1}{2r_{23}r_{13}^3 r_{12}^3} - \frac{3}{2r_{23}r_{13}r_{12}^5} - \frac{1}{2r_{23}^3 r_{13} r_{12}^3}\right) \quad (4.3.3)$$

here, the term $C_7 = 604.96\ meV\text{Å}^7$ comes from the induced dipolar polarizabilities α_{He}.

Finally, the complete description of the trimer interaction including the many-body correction takes the form:

$$V_{3B}(r_{12}, r_{13}, r_{23}) = V_{2B}(r_{12}, r_{13}, r_{23}) + V_{\mu\mu}(r_{12}, r_{13}, r_{23}) \quad (4.3.4)$$

In order to represent the pairwise interacting three-body potential V_{2B} (4.3.1), the many-body corrected three-body potential V_{3B} (4.3.4) and the polarization correction $V_{\mu\mu}$ (4.3.3), the contours of the four-dimensional PES for these two configurations are plotted.

To make the representation easier to analyse, and taking as reference **Fig. 4.6**, the He(1) and $Li^+(3)$ system is fixed to a minimum interatomic distance $r_{13} = 1.91$ Å, while the

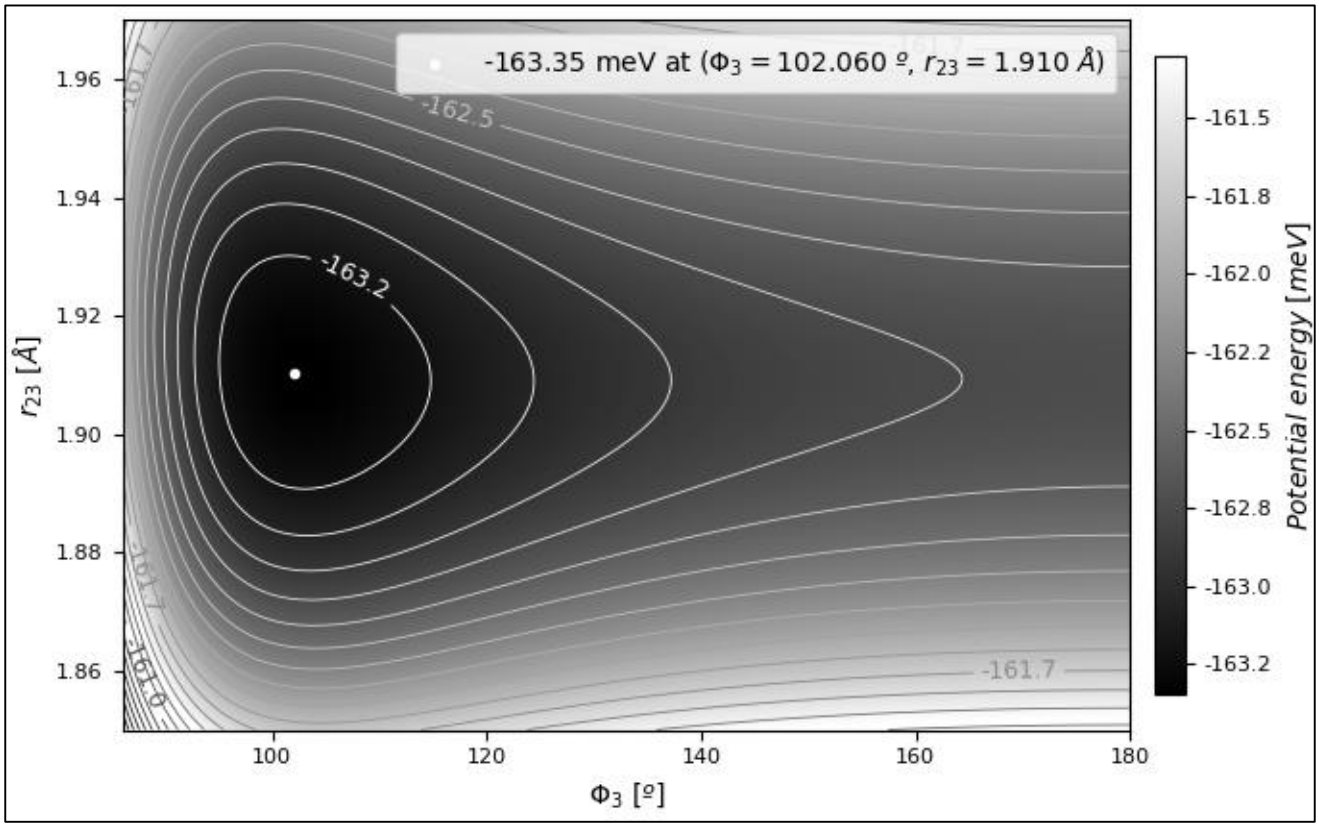

Fig. 4.7 Classical PES of the ^{4}He-^{4}He-Li^+ system calculated with the V_{2B} term (4.3.1).

[7] The procedure to obtain this expression is not trivial.

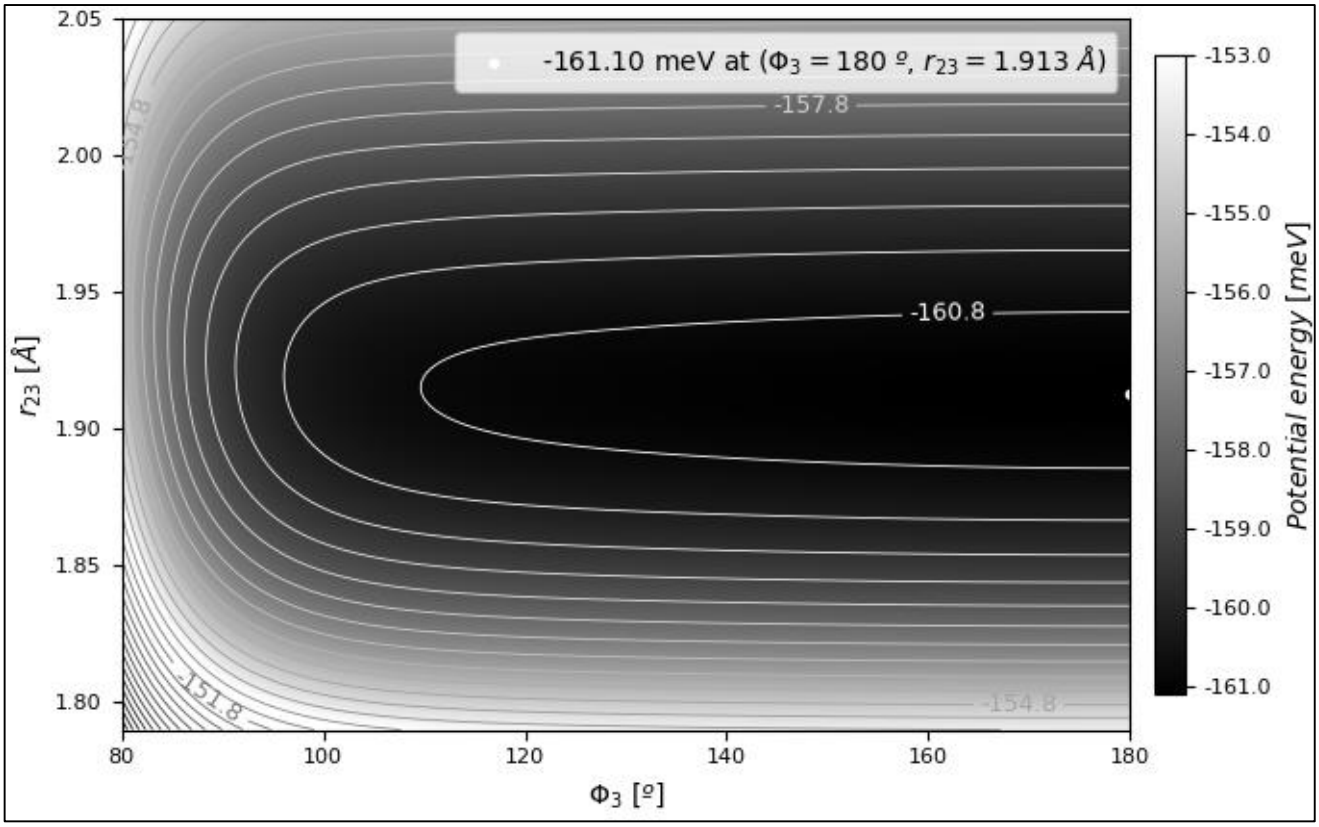

Fig. 4.8 PES of the ^{4}He-^{4}He-Li$^+$ system corrected for the three-body deformation energy.

distance r_{23} between the Li$^+$(3) and He(2) is allowed to vary over a small range. As for the He dimer, r_{12} is trigonometrically expressed in terms of the angle ϕ_3 which is bound to the interval $[80º, 180º]$.

The V_{2B} PES is shown in **Fig. 4.7**. The most notable characteristic is that the minimum energy of the system, which is $V_{2B} = -163.35\, meV$, takes place at the minimum pairwise interatomic distances for both the He dimer and the He(2)-Li$^+$(3) system, respectively $r_{12} = 2.97$ Å $(\phi_3 = 102.1º)$ and $r_{23} = 1.91$ Å. This result was to be expected, given that the many-body correction was not included the pairwise minimum potential energies have emerged.

The V_{3B} PES is featured in **Fig. 4.8**. Firstly, in comparison to the V_{2B} PES, the minimum energy configuration has been displaced to $\phi_3 = 180º$ and its value has changed to $V_{3B} = -161.1\, meV$. The PES of the dipole-dipole interaction term (4.3.3) is shown in **Fig. 4.9.** It introduces a repulsive correction of $V_{\mu\mu} = 2.24\, meV$ to the

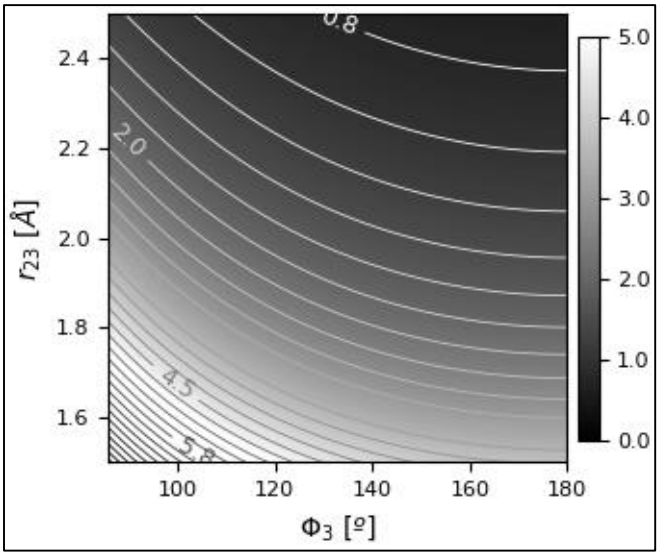

Fig. 4.9 Repulsive correction that emerges from the dipole-dipole interaction term (4.3.3).

minimum energy of the system, which corresponds to a 1.4% increase over the pairwise interaction potential energy V_{2B}. It is noticeable that the polarization correction decreases slightly in potential energy with the increase in angular separation ϕ_3 between the He atoms, and more prominently with the increase of interatomic distance r_{23}, effectively displacing the equilibrium geometry from a triangular to a linear geometry.

Secondly and finally, the effect of the dipole-dipole interaction term has introduced a change to the equilibrium interatomic distances of the He dimer and the He(2)-Li^+(3) system, which are now considerably different from their pairwise equilibrium positions. These distances have become $r_{12} = 3.823$ Å and $r_{23} = 1.913$ Å.

5 Conclusions

The study that was initially conducted regarding the physical basis of the intermolecular forces of interaction between atoms and molecules as well as the formalism for their representation and the methods that have been historically employed, following the discussions presented by A. Stone in [1], has allowed the successful application of these concepts to study the potential energy curves and surfaces of different physical systems, effectively modelling the energies of interaction for real systems. As an introduction to this field of research, this project has provided valuable knowledge.

As for the results obtained, several conclusions can be drawn:

The Tang-Toennies PECs for the homogeneous rare-gas dimers seen in **Fig. 4.1** and **Fig. 4.2** that were calculated in the present study have been shown to agree exactly with recent *ab initio* results obtained by Tang and Toennies [3]. It is altogether the most accurate potential model that has been employed in the present work.

Concerning the Pirani or Improved Lennard-Jones potential, the PECs from **Fig. 4.3** and **Fig. 4.4** have been traced with the parameters set by Pirani *et al.* [4] and those results were contrasted with their own first principles calculations. The overall behaviour of the Pirani potential is confirmed in the present study as a valid approach to homogeneous rare-gas dimers, particularly for the He_2, Ne_2, Ar_2, Kr_2 and Xe_2 dimers, as well as for He-Li^+ systems. The

different choices in the β factors in all cases except for the He_2 dimer have been made by the author of this study in search for better agreement with the TT potential model.

As reported from *ab initio* calculations by Soldán *et al.*, their potential model is a better fit altogether and thus an improvement over the Pirani or ILJ potential for representing the He-Li^+ interaction. In their study [6], they reported a calculated interatomic energy of $-80.47\ meV$ for an equilibrium interatomic distance of 1.9 Å at a high level of theoretical precision. However, using the same potential model and the coefficients they provide, the minimum well depth and position reached are $-78.257\ meV$ and 1.89 Å. This deviation suggests an error in the parameters provided, however such error has not been uncovered during the present work.

Finally, the three-body PES calculations require additional commentary. The equilibrium position angle $\phi_3 = 102.72º$ was calculated by Liu *et al.* [9], yet this is slightly different from what was obtained for the V_{2B} PES, shown in **Fig. 4.7,** which was $\phi_3 = 102.06º$. This deviation is corrected when an interatomic distance $r_{13} = 1.908$ Å is chosen for the He(1)-Li^+(3), suggesting that the classical calculation for such interatomic distance can be further improved. Aside from this slight difference, many first principles calculations have shown partial agreement with the results shown in the present study, again reported in [9].

Moreover, the equilibrium geometry of the three-body system shown in **Fig. 4.8** is altered significantly by the dipole-dipole correction and the pairwise interatomic equilibrium distances vary further. The change to the He dimer minimum position can be explained from the change in equilibrium geometry of the trimer system, however the change to the He(2)-Li^+(3) interatomic distance, which became $r_{23} = 1.913$ Å, is indicative of theoretical deficiencies in the simple model that was employed. Altogether, it is obvious that Quantum Mechanical considerations are necessary to arrive at precise calculations of the equilibrium geometry of the He-He-Li^+ trimer.

6 Acknowledgments

The proficiency in knowledge necessary for this *End of Degree* Project was acquired thanks to the continued work of the professors at La Laguna University whom have imparted classes to the author.

This study reached its final stage through the upstanding guidance, support and advice of Prof. José Diego Bretón Peña. All bibliographical materials and the overall structure of the project were also provided by him.

7 References

Provisional access to the Python code developed for the project has been made available for any ULL account.

[1] A. Stone. The Theory of Intermolecular Forces, 2nd Edition, Oxford University Press, 2013.

[2] C. Cohen-Tannoudji, B. Diu, F. Laloë, Quantum Mechanics, Vol. 2, Wiley.

[3] K. T. Tang and J. P. Toennies, **J. Chem. Phys.**, Vol. 118, No. 11, p. 4976, (2003).

[4] F. Pirani, S. Brizi, L. F. Roncaratti, P. Casavecchia, D. Cappelletti and P. Vecchiocattivi, **Phys. Chem. Chem. Phys.**, Vol. 10, No. 36, p. 5477, (2008).

[5] A. Erdélyi, W. Magnus, F. Oberhettinger and F. G. Tricomi, Higher Transcendental Functions, vol. II, McGraw-Hill (1953).

[6] P. Soldán, E. P. F. Lee, J. Lozeille, J.N. Murrell and T. G. Wright, **Chem. Phys. Letters**, Vol. 343, p. 429, (2001).

[7] S. G. Porseva and A. Dereviankob, **J. Exp. and Theo. Phys.**, Vol 102, No. 2, p. 195 (2006).

[8] G. Maroulis, A.J. Thakkar, **J. Chem. Phys.**, Vol. 89, p. 7320, (1988).

[9] M. Liu, M. Wu, H. Han, T. Shi, **J. Chem. Phys.**, Vol. 145, 34304, (2016).